J. Mater. Eng. (1991) 13:119–127


# Metallic Glasses in Distribution Transformer Applications: An Update[1]

V.R.V. Ramanan

**Abstract.** Metallic glasses suffer substantially lower energy losses than their crystalline counterparts and, therefore, allow increased efficiencies of operation in transformers. This challenge posed by metallic glasses to the use of conventional, crystalline silicon steels as core materials in the manufacture of electrical distribution transformers has found increased recognition, internationally, among manufacturers and users of such transformers. This paper provides an update on the understanding of the behavior of these materials. The focus will be on the properties of Fe-rich metallic glasses, particularly the Fe–B–Si glasses, as these offer excellent soft magnetic characteristics and economic viability. The core loss characteristics of these materials will be discussed in some detail; a recent model for the loss mechanism will be reviewed. Results on the aging behavior of these metallic glasses will be presented, along with a model describing the aging behavior. Finally, the tendency of these materials to lose ductility following anneals will be addressed.

## Background

The advantageous soft magnetic characteristics of metallic glasses, low magnetic anisotropy, high resistivity and, therefore, lower coercivities and core losses over a wide range of frequencies, are well documented. Of the variety of applications for these materials, the largest volume usage, by far, both in dollars and tonnage, is in cores of electrical distribution transformers. Allied-Signal's first commercial alloy for these applications was METGLAS® 2605S-2 [1], an Fe–B–Si ternary alloy. The stability of the metastable glassy state, and the stability of the soft magnetic properties obtained in that state, over the projected lifetime of an electrical distribution transformer, were the major initial concerns of transformer core designers. The knowledge accumulated indicates that these concerns should not exist for the Fe–B–Si alloys.

It may safely be said that the advent of Fe–B–Si metallic glasses has been the most important advance in materials for the cores of transformers in the electrical power distribution system since the introduction of Goss texture in crystalline silicon steels. Consequently, this alloy system has been studied exhaustively. The commercial significance of metallic glasses in this system is underscored by the rather furious activity revealed in the patent literature.

Metallic glasses, in their as-cast state, have high quenching stresses resulting from the very rapid cooling rates employed to prepare these materials which, in turn, tend to mask the advantageous soft ferromagnetic properties realizable in these materials. Consequently, annealing of metallic glasses is a necessary step prior to their use in almost any application. Such annealing serves to relax the quenching stresses, and, in the presence of externally applied magnetic fields, is often used to induce a preferred axis of magnetization in the glassy material. For the purposes of distribution transformer applications, this axis lies along the ribbon length, the axis along which the core will be excited during the application. The domain structure in the annealed alloy consists mostly of plane parallel 180 deg domain walls. The nominal

[1] This paper is excerpted from a paper delivered at the Workshop on Amorphous Core Transformers held in May 1990 at New Delhi, India.

The author is with the Metals and Ceramics Laboratory, Allied-Signal Inc., P.O. Box 1021R, Morristown, NJ 07962, USA.

"optimal" anneal conditions for METGLAS 2605S-2 are: 380°C, 2 hr, with 800 A/m external field applied along ribbon length.

## Core Loss Mechanisms

Traditionally, it has been convenient to separate the total core loss obtained from a ferromagnetic material into two major components, referred to as the hysteresis and eddy current contributions. For a given maximum induction level, the hysteresis and eddy current components have linear and quadratic dependencies on the magnetizing frequency, respectively. A power law also characterizes the dependence of the losses on the induction level for a given frequency. The exponents in this case are about 1.7 and 2 for the hysteresis and eddy current components, respectively.

The eddy current component itself is separable into two parts, customarily referred to as the "classical" and "excess" eddy current components. Both of these components are due to Joule heating ($i^2R$ losses) associated with internal currents generated by the varying magnetization of the material. The classical component refers to the rate of magnetization change in a uniformly magnetized material, and does not acknowledge the existence of ferromagnetic domains. The excess eddy current losses are a direct consequence of the presence of domains and arise from currents localized at the domain walls. Introducing the symbol $P$ to represent the core loss *per cycle* (J/kg), the above discussion may be summarized as follows:

$$P_T = P_h + P_{cl} + P_{ex} \qquad (1)$$

where the subscripts $T$, $h$, $cl$, and $ex$ denote total, hysteresis, classical eddy current, and excess eddy current, respectively; $P_h$ is independent of frequency. The classical eddy current loss is given by the expression:

$$P_{cl} = [(\pi B_m t)^2 f]/(6D\rho) \qquad (2)$$

where $t$ is the thickness, $D$ the density, and $\rho$ the electrical resistivity of the material. In the case of METGLAS 2605S-2, $t$ = 25 μm, $D$ = 7.2 g/cc, and $\rho$ = 1.28 μΩm, so that at 60 Hz and 1.4 T, for example, $P_{cl}$ is about 14 μJ/kg, which is a negligible fraction of $P_T$, which is about 3 mJ/kg (see Fig. 1). As will be shown later, such is not the case with conventional, crystalline transformer core materials, where the classical eddy current loss is a substantial

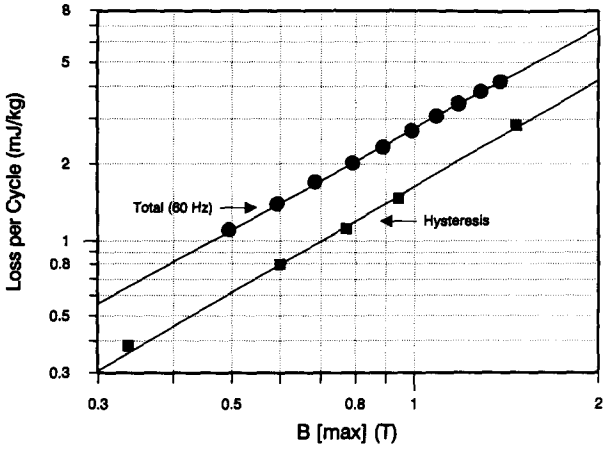


**Fig. 1.** Total loss per cycle at 60 Hz and hysteresis loss as a function of the maximum induction level, for METGLAS® 2605S-2.

fraction of the total loss, primarily because of much lower resistivity.

The measured behavior of $P_T$ at 60 Hz and $P_h$ are shown in Figure 1 as a function of the maximum induction, $B_m$, for a toroidal core of METGLAS 2605S-2. Approximately one-half of the total loss is found to arise from hysteresis losses. Since the classical eddy current component is negligible in metallic glasses, excess eddy current losses account for the other half of the total loss. This is a substantial fraction, when comparisons are made with silicon steels. However, the absolute values for the excess eddy current component are much lower than in the crystalline materials.

The most used model, to date, for describing $P_{ex}$ in terms of domain wall dynamics is the Pry and Bean (P-B) model [2]. Here, plane parallel domain walls, parallel to the magnetizing direction and evenly spaced through the sample, are assumed to move with equal velocities upon magnetization. This model predicts that

$$P_{ex} = P_{cl} \times (1.628\, d/t) \qquad (3)$$

where $d$ is the uniform width of domains prior to magnetization.

The core loss versus frequency data in Figure 2, derived from the same core as in Figure 1, illustrate that the postulate of the regular domain structure in the P-B model does not represent a "real" material. Clearly, the expected straight line is not obtained. This kind of behavior is also seen in silicon steels. The departure from ideality in a "real" material lies primarily in the fact that there are pinning sites for the domain walls ascribable to inhomogeneities.

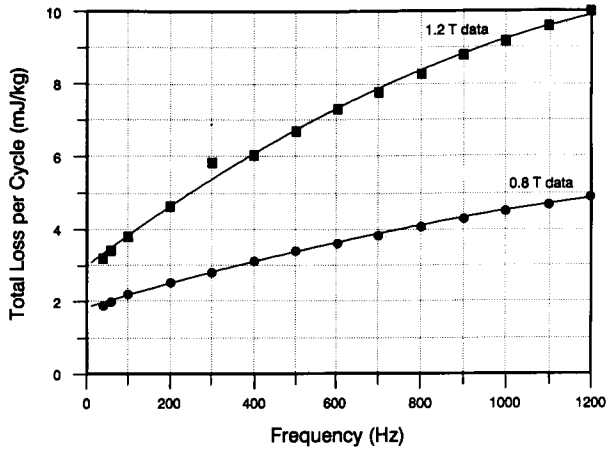


**Fig. 2.** Total core loss per cycle as a function of frequency, for METGLAS 2605S-2 at two different maximum induction levels.

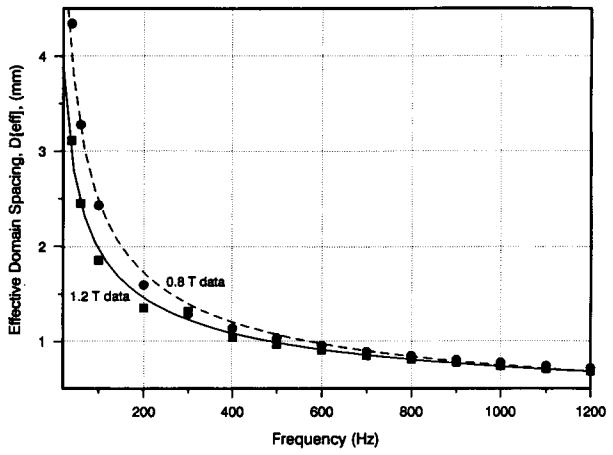


**Fig. 3.** Behavior of the effective domain width, $d_{eff}$, vs. frequency.

However, Eq. (3) does offer some insight into the magnetization process.

The calculated values for $P_{ex}$ may be used to evaluate an "effective" domain width, $d_{eff}$, from Eq. (3). In the ideal case (P-B model), this quantity will be independent of frequency. The behavior of $d_{eff}$ versus $f$ for METGLAS 2605S-2 is shown in Figure 3, as derived from the data presented in Figures 1 and 2. The rather large values for $d_{eff}$ at low frequencies indicate that only a fraction of domain walls are participating in the magnetization process. In the language of the P-B model, this $d_{eff}$ may be viewed as the spacing between *participating* domain walls. The inactive domain walls in the material are "pinned," or restricted from motion. The low frequency data in this figure for 0.8 T imply that a smaller number of pinning sites have been overcome, leading to a higher $d_{eff}$. As the frequency increases, the $d_{eff}$ asymptotically approaches a value $d_{final}$, which is probably the true domain spacing in the material. Scanning electron microscopy reveals that the domain width in as-annealed METGLAS 2605S-2 is 0.5–1 mm, consistent with Figure 3. The fact that $d_{final}$ is the same for all $B_m$ indicates that all the walls are active at high enough frequencies. The real departure from the P-B model is at low frequencies.

Recently, an improved model for the description of $P_{ex}$ has been proposed by Bertotti et al. [3,4]. This model has been shown to apply well to data from silicon steels, whether oriented or not, and the "predictive" capabilities of the model for grain oriented steels has been demonstrated [4]. For the case of METGLAS 2605S-2, the Bertotti model accurately describes the qualitative features of excess eddy current loss observed in experiment.

In this model, the magnetic material is pictured as a collection of "magnetic objects" (MO). Each of these objects, given the right conditions, contributes to the magnetization process. These objects could range from clusters of atoms with similar responses to magnetic fields to entire grains in fine grained materials, such as in nonoriented steels. They could also be domain walls. In fact, it is convenient to picture the MO as comprising domain walls and the "potential wells" they reside in; these potential wells contain information on the pinning site and strength distribution governing the response of the corresponding wall. Through the postulation of a statistical distribution of local coercive fields, an analysis, at a given induction level and frequency, is then carried out on the magnetization response of this collection of MO. The main results of the model may be summarized via the following equations:

$$H_{ex} = (P_{ex}/4B_m) \tag{4}$$

$$H^{(w)} = (4GSB_m f/\rho) \tag{5}$$

$$\tilde{n} = (H^{(w)}/H_{ex}) \tag{6}$$

$$\tilde{n} = \tilde{n}_0 + (H_{ex}/V_0) \tag{7}$$

where $G$ is a constant that may be approximated by 0.136; $S$ is the cross-sectional area of the material; $\tilde{n}$ is the number of simultaneously active MO placed randomly through the cross-section; $\tilde{n}_0$ is $\tilde{n}$ at $f = 0$; and $V_0$ is a parameter related to the coercivity distribution.

Equations (4) and (6) are definitions of the respective quantities. Consequently, the "field" $H^{(w)}$ in Eq. (5) represents the excess field in the case

where the entire flux rate is concentrated in a single magnetic object. It is intuitively obvious that $\bar{n}$ should be a function of $H_{ex}$; the linear relationship posed in Eq. (7) has been found to describe a variety of crystalline materials [3]. Physically, the constant $V_0$ may be pictured as the average, minimum difference in coercivity between two magnetic objects. If, and only if, the linear relationship holds, the algebra then leads to the dependence of $P_{ex}$ on $B_m$ and $f$:

$$P_{ex} \propto B_m^{1.5} \times f^{0.5} \tag{8}$$

Recalling how $d_{eff}$ was calculated, it may be seen that Eq. (8) is equivalent to

$$d_{eff} \propto (B_m f)^{-0.5} \tag{9}$$

As illustrated in Figure 4, Eq. (9) describes the metallic glass core of Figures 2 and 3 very well. In this figure, the $d_{eff}$ data from three induction levels, 0.8, 1.0, and 1.2 T, calculated as for Figure 3, have been plotted. The slope of the fitted line in this figure reproduces the exponent of −0.5. The Bertotti model has thus satisfactorily explained the observed core loss characteristics in METGLAS 2605S-2. Metallic glasses from other alloy systems do not seem to obey Eq. (7) [3] and, consequently, Eq. (8) is invalid.

In METGLAS 2605S-2, the quantitative fit of the model to data is, however, not as satisfactory, and the model needs some fine tuning. This is illustrated in Figure 5. In this figure, Eq. (7) has been plotted, using the experimental values for $\bar{n}$ calculated from Eqs. (4) and (5), per the definition in Eq. (6). Data at 0.8, 1.0, and 1.2 T from each of three cores of

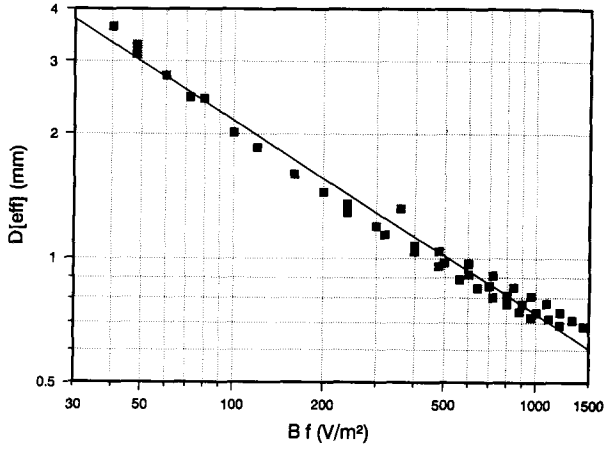


**Fig. 4.** Data of Fig. 3 fitted to the Bertotti model [see Eq. (9) in the text]. Data from $B_m$ = 1.0 T are additionally included.

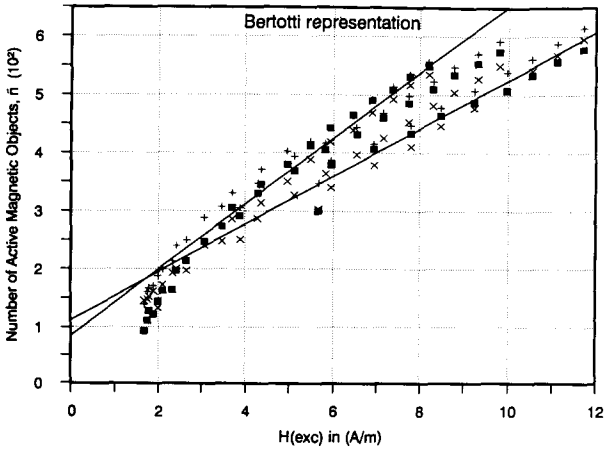


**Fig. 5.** A plot of the linear relationship of Eq. (7) in the text. Data at 0.8, 1.0, and 1.2 T from each of three different cores of METGLAS 2605S-2 are included.

METGLAS 2605S-2, prepared from ribbon thicknesses ranging between 20 and 23 μm, are represented in this figure. The correspondence between the model and experiment is not good at low $H_{ex}$ (frequencies less than about 100 Hz). When the data above 100 Hz are fitted to Eq. (7), the values for $V_0$ evaluated from each set of data (induction level and source core) fall within the range 0.021 ± 0.003 A/m. The intercepts, $\bar{n}_0$, however, fall within 77 ± 33, a very broad range.

The value for $V_0$ of 0.02 A/m (0.25 mOe) seems reasonable, and is much lower than the 0.13 A/m found for oriented steels [3,4], indicative of the greater ease in magnetizing a metallic glass. The dependence of $\bar{n}_0$ on $B_m$, and the physical significance of the departure of data from the linear relationship of Eq. (7) at low frequencies, are areas which need to be addressed.

## Comparison with Crystalline Materials

The core losses ("no-load" losses) obtained from metallic glasses are about one third of those obtained from conventional, grain oriented 3 wt% silicon steels. There are, primarily, two reasons for this improvement. First, metallic glasses are easily magnetizable, because of the lack of crystalline anisotropy and the low magnitudes of induced anisotropy. As a result, the permeability is higher and the coercivity is lower in metallic glasses. The dc coercivity in properly annealed METLGAS 2605S-2, for example, is about 1.6 A/m (20 mOe), which is a fifth of that of the silicon steels. Consequently, the hysteresis component of the total core loss is correspondingly lower.

Second, the resistivity of metallic glasses is about an order of magnitude higher than in silicon steels, again a consequence of the random atomic arrangement. In addition, metallic glasses are intrinsically thin. The eddy current losses should therefore be correspondingly lower [see Eqs. (2) and (3)]. However, because of the greater domain wall spacing, some of these gains are surrendered by metallic glasses [Eq. (3)]. The discussion above is highlighted by Figure 6, which offers a comparison of the various core loss components in a variety of silicon steels and in METGLAS 2605S-2. The major gains in the metallic glass are in the hysteresis and classical eddy current components.

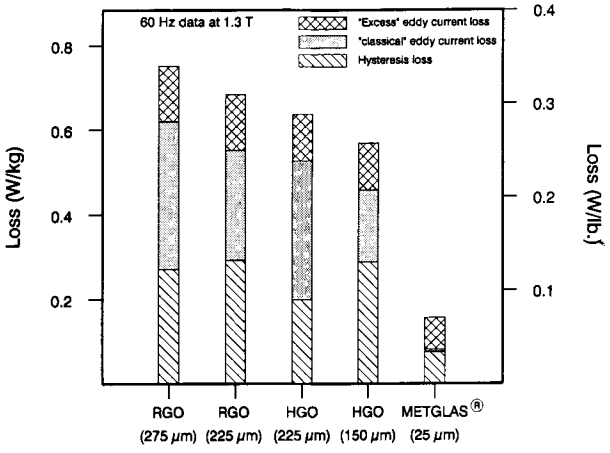


**Fig. 6.** Comparison of the magnitudes of the individual components of total core loss in a variety of transformer core materials [16]. (RGO: regular grain oriented silicon steel; HGO: highly grain oriented silicon steel.)

**Table 1.** Core Loss Comparison (W) of a Wide Range of Electrical Distribution Transformers, with Different Core Materials[a,b]

| kVA | AM | Current SS | SS in Service |
|---|---|---|---|
| Single Phase | | | |
| 10 | 12 | 33 | 65 |
| 15 | 14 | 40 | 80 |
| 25 | 15 | 57 | 100 |
| 50 | 29 | 87 | 210 |
| 75 | 39 | 130 | 260 |
| 100 | 49 | 160 | 320 |
| Three Phase | | | |
| 75 | 51 | 184 | 360 |
| 150 | 79 | 280 | 510 |
| 300 | 167 | 516 | 1000 |
| 500 | 225 | 690 | 1400 |
| 750 | 315 | 900 | 1800 |

[a] Data from General Electric Co. [15].
[b] AM = amorphous metal. SS = silicon steel.

Under the auspices of a variety of commercialization programs in the United States, single-phase and three-phase distribution transformer cores with a wide range of kVA ratings have been built using METGLAS 2605S-2 as the core material. The typical performance characteristics of these transformers are compared in Table 1 against those of comparable transformers with silicon steel cores, using data from General Electric (GE). Metallic glasses clearly offer improved transformer efficiencies.

## Embrittlement in Annealed Metallic Glasses

The terms "ductility" and "embrittlement" in metallic glasses refer to deformation modes such as bending or rolling. As such, in a tensile test, failure occurs coincident with yielding and the macroscopic ductility is equivalent to the elastic strain to failure. In the engineering sense, this is "brittle" behavior. When this plastic instability is avoided, as in bending or rolling, macroscopic deformation is evidenced in a multiplicity of intense local shear bands, the true strains in which can be of the order of 10 [5]. However, as a consequence of the necessary anneals of metallic glasses, these materials suffer a substantial loss in their as-cast ductility. This is particularly true of Fe based metallic glasses.

It is apparent from a review of research on this phenomenon that the mechanism for the loss in ductility remains speculative. Effects due to impurity elements [6], phase segregation effects [7] and the rate of dissipation of "free volume" from the as-quenched glass ("stress relaxation") [8] have all been cited as causes. However, it does seem safe to say, at least in the case of Fe based glasses, that the loss in ductility correlates with stress relaxation in the metallic glass as it is annealed [6]. Precipitous losses in ductility are found to occur when METGLAS 2605S-2 begins to approach its fully relaxed state [9]. Much more work is needed for a clear understanding of this subject.

In the case of Fe–B–Si glasses there does seem to be an effect of the alloy chemistry on the ductility behavior, as illustrated in Figure 7. The fracture strain was measured on ribbons of the various chemistries, after they were subjected to an anneal at 360°C for 90 min. (The fracture strain is defined by the relation $[t/(d - t)]$, where $t$ is the ribbon thickness and $d$ is the "bend–break" diameter given by the separation between two parallel platens at the point where a

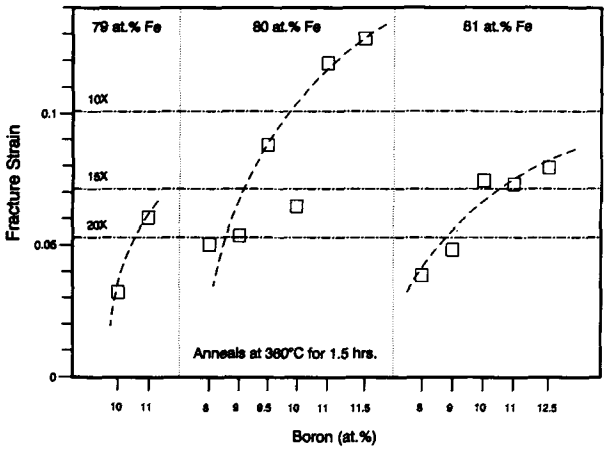


**Fig. 7.** Fracture strains measured on various Fe–B–Si alloys following anneals at 360°C for 1.5 hr. The horizontal lines marked 10X, etc., represent, for reference, the bend–break diameter as a multiple of the ribbon thickness.

strip of metallic glass fractures as it is being bent. Better ductility is indicated by a greater fracture strain, that is, the annealed ribbon may be bent to a smaller diameter prior to fracture.) As noted from this figure, the fracture strain is seen to increase as the B content increases from 8 to 11.5 at%, for a given Fe content.

## Aging Behavior

The mechanisms by which the magnetic properties of silicon steels change with age are reasonably well understood, and quantified [10]. The principal aging effects arise from interstitial migration and grain boundary precipitation. Impurities, particularly carbon, play a major role. Manufacturers of these materials have learned impurity control as a consequence. Metallic glasses do not have this wealth of data behind them, in spite of the considerable effort that has been directed, in recent years, at generation of aging data and at understanding the aging behavior of these metastable materials. The outlines of a quantitative understanding have emerged, and what has been learned indicates that the mechanisms for aging of metallic glasses are distinct from those of silicon steels.

Changes in a variety of seemingly unrelated mechanical and magnetic properties of metallic glasses are governed by a log time kinetic, suggesting a fundamental unity. In other words, the properties change linearly with the logarithm of time, a behavior indicative of a distribution of activation energies. Such a dependence is entirely different from the kinetics of thermally activated processes which may be described by a single activation energy. Although there is work in progress aimed at quantifying the atomic level mechanisms responsible for aging, or relaxation, of metallic glasses, it is easy to rationalize the existence of a spectrum of activation energies available in these materials.

Even in crystalline ferromagnets different relaxation mechanisms exist. Short term, and usually reversible, effects such as disaccommodation arise from local rearrangements of small atomic clusters around domain walls, and effects such as diffusion, with much higher activation energies, govern long term aging characteristics. These exemplary thermally activated processes dominate at distinctly different temperatures. Precisely such processes must exist in metallic glasses too. A spread in energy for the relaxation processes is to be expected because of the amorphous structure: The lack of a well-defined crystallographic symmetry, or bonding, implies the existence of many atomic clusters, each of which must have many nearly degenerate local structural states available. Single atom processes, such as diffusion, are also available, at the high end of the activation energy spectrum, and eventually result in the crystallization of the material. It is firmly established that bulk crystallization itself may be ruled out as a contributor to the aging behavior in metallic glasses at typical device operating temperatures; the integrity of the glassy structural state is very high.

The log time ($t$) kinetic for relaxation in metallic glasses has been mathematically quantified by Gibbs et al. [11] through their activation energy spectrum (AES) model, using a formalism originally developed by Primak [12]. The principal postulate in this model is that at a given temperature $T$, there exist processes involving the rearrangement of atoms or groups of atoms, characterized by a spectral density function, that is, a function $Q(E,T,t)$ describing the number density of available relaxation processes with an activation energy $E$. This function comprises two parts: $q_s(E,T)$, a time independent equilibrium component, and a nonequilibrium component, $q(E,T,t)$, controlling the aging behavior. The equilibrium component defines the initial state of the material.

The time dependence in the nonequilibrium component is explicitly separated, and characterized along the lines of a chemical rate equation, acknowledging that the processes are, indeed, thermally activated. Accordingly, the change in a property, $\Delta P$, which

will have occurred after isothermal annealing for a time $t$ at temperature $T$ is given by the equation:

$$\Delta P = \int c(E)q(E,T) \cdot [1 - \exp(-\nu_0 t[\exp(-E/kT)])]\, dE \quad (10)$$

In this equation: $c(E)$ is a coupling function, presumed to be temperature independent, relating the occurrence of a process of activation energy $E$ to the consequential change in the measured property; $\nu_0$ is an attempt frequency; and $k$ is the Boltzmann constant. The expression in oversize brackets is called the annealing function, after Primak.

Assuming that the product $c(E)q(E,T)$ varies slowly on an energy scale of $kT$, integration of Eq. (10) reveals that the change in $P$ is locally linear in the logarithm of time, the experimentally observed behavior. A variety of functions $q(E,T)$ have been employed for the analysis of experimental data. A Gaussian function seems to fit structural relaxation data very well [13]. However, the simplest application of the model is most illustrative in terms of explaining the aging curve. In this application [11], the product $c(E)q(E,T)$ is assumed to be a constant over a given energy interval and zero elsewhere, that is, a "box" spectrum, and the annealing function is approximated by a step function at an energy $E_0$ given by:

$$E_0 = kT \ln(\nu_0 t) \quad (11)$$

Then, the change in property after time $t$ at temperature $T$ is given by

$$\Delta P = \text{const.} \times kT \ln(\nu_0 t) \quad (12)$$

A discussion of the physical significance of the attempt frequency is in order. It is commonly assumed to be of the order of the Debye frequency, which is a reasonable scale for most single-atom processes. For multiatom processes, such as relaxation of clusters, an entropy term has to be included which will modify this frequency. In other words, the attempt frequency has a temperature dependence.

The implication of these approximations is that no processes with activation energies greater than $E_0$ and all those with activation energies less than $E_0$ will have taken place by time $t$ at temperature $T$. As a result, at a given temperature, property changes occur only after a time $t$ corresponding to the lowest energy of the spectrum, and then proceed linearly in the logarithm of time. In reality, the above step function is blurred over the range of a few $kT$, so that small property changes may be noted prior to the onset of "serious" changes in property.

This is precisely the behavior observed in the core loss of METGLAS 2605S-2 as it is aged. The aging characteristic of this Fe–B–Si alloy is shown in Figure 8, in a plot of the fractional change in core loss (with respect to that at time zero) against time at various aging temperatures. Small initial property variations are followed by more rapid changes in core loss, and linearity in the logarithm of time is clearly observed at all temperatures. A systematic change in the slope of this behavior is also evident as a function of the isothermal aging temperature. Most of the data in this figure are from [14]. To generate this data, a series of optimally annealed toroidal cores of the alloy were aged at the noted temperatures. The core losses were measured at room temperature following the residence of the cores at the aging temperature for various time intervals. Thus, the aging time in Figure 8 is actually the cumulative residence time at temperature. The heating and cooling cycles between room temperature and the aging temperature each consumed about 30 min. The cores were excited to about 1.4 T at 60 Hz when at aging temperature.

The basic validity of the simplest AES model allows one to predict the core loss changes to be expected of this commercial metallic glass product at typical transformer operating temperatures in the range of 100–125°C. It should be appreciated that, as a matter of practical convenience, actual aging data have to be collected at higher temperatures

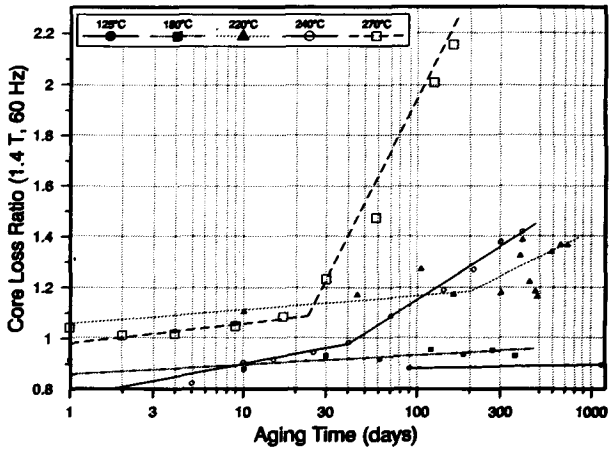


**Fig. 8.** Behavior of 60 Hz, 1.4 T core loss of METGLAS 2605S-2, as a function of aging time at various temperatures.

("accelerated" aging tests); for example, there is little change in core loss after about 1200 days at a relatively "high" 180°C (Fig. 8).

Assuming a value of $10^{12}$ Hz for the attempt frequency, the onset time of about 40 days for aging at 240°C (see Fig. 8) corresponds to an $E_0$ of about 1.8 eV. In turn, the onset time for aging at 220°C is predicted to be about 225 days, which is seen to be reasonably accurate from Figure 8. The observed behavior at 270°C (onset at about 15 days, as opposed to the four days predicted by the lower temperature data) suggests a change in the character of relaxation processes; multiatom clusters are most certainly involved, and the assumption in the AES model of noninteracting relaxation processes begins, perhaps, to break down.

Although precise calculations of property changes may be made for a given temperature from the AES model, as in [13], reasonable forecasts of expected property behavior may be made using available data and Eqs. (11) and (12). The self-consistent data at 240°C and 220°C will be used below for the estimation of the performance of METGLAS 2605S-2 at even lower temperatures.

Using the value $10^{12}$ Hz for the attempt frequency, it may be seen from Eq. (11) that if the onset of degradation in core loss is to occur, say, after 30 years at 125°C, degradation should have commenced after 31 days, 5.3 hr, and 40 min at 180°C, 240°C, and 270°C, respectively. None of this is borne out by experiment. Conversely, the onset time of 40 days determined from data at 240°C would predict that degradation will commence at 125°C after about *24,900 years*! Finally, assuming worst case situations (many of them unrealistic or unphysical): that the attempt frequency depends seriously on temperature and changes from about $10^{11}$ Hz at 270°C to about $10^{13}$ Hz at 125°C; that onset of degradation commences after 1 day at 270°C (slowly varying portion in Fig. 8); and, that the slope of the core loss change at 125°C will be the same as in the rapidly varying portion in Figure 8 for 270°C (about 0.1 in the units of that figure); then, the core loss of METGLAS 2605S-2 will degrade by 10% after 30 years at 125°C, with the onset of degradation commencing at 11 years.

In spite of the fact that "real" transformers are different from laboratory cores, in terms of assembly and core performance environment (overloads, etc.), the current state of the understanding of aging behavior of metallic glasses indicates that amorphous metal cored electrical distribution transformers will be stable over the lifetime of a typical working transformer. Preliminary data from various utilities confirm this. San Diego Gas and Electric Co., for example, randomly selected 21 amorphous metal cored transformer units (25 kVA), from a total of 210 such units installed, for testing after a period of 18 months in the field. In many of the units, the no-load loss decreased [17]. The maximum increase noted was about 0.3 W in a unit with an initial no-load loss of about 18 W; the average increase was about 0.1 W. About 1000 25 kVA units manufactured by GE, installed by various utilities about five years ago under a program sponsored by the Electric Power Research Institute (EPRI), have not shown any cause for concern regarding aging.

## Conclusions

Metallic glasses bring substantially lower core losses to electrical distribution transformers. The reasons for their low losses are reasonably well understood, and a more fundamental understanding of the core loss mechanisms is emerging. The activation energy spectrum model describes well the experimentally observed aging behavior of metallic glasses. Consequently, concerns regarding the stability, over time, of the properties of these materials are alleviated. Today's commercial metallic glass product satisfies all current requirements, both in terms of properties and their stability over time, of electrical distribution transformer manufacturers for their core material.

## References


1. METGLAS® is the registered trade name of Allied-Signal Inc. for amorphous alloys of metals.
2. R.H. Pry and C.P. Bean: *J. Appl. Phys.*, 1958, vol. 29, p. 532.
3. G. Bertotti: *IEEE Trans. Magn.*, 1988, vol. MAG-24, p. 621.
4. G. Bertotti, F. Fiorillo and G.P. Soardo: *IEEE Trans. Magn.*, 1987, vol. MAG-23, p. 3520.
5. T. Masumoto and R. Maddin: *Acta Met.*, 1971, vol. 19, p. 725.
6. D.M. Kroeger, G.S. Canright, C.G. McKamey, D.S. Easton and J.O. Scarbrough: *Acta Met.*, 1987, vol. 35, p. 989.
7. J. Piller and P. Haasen: *Acta Met.*, 1982, vol. 30, p. 1.
8. T.W. Wu and F. Spaepen: *Mechanical Behavior of Rapidly Solidified Materials*, S.M.L. Sastry and B.A. McDonald, eds., p. 293, The Metallurgical Society, Warrendale, Pennsylvania, 1986.
9. H.H. Liebermann, J. Marti, R.J.J. Martis and C.-P. Wong: *Met. Trans. A*, 1989, vol. 20, p. 63.
10. W.C. Leslie and D.W. Stevens: *Trans. ASM*, 1964, vol. 57, p. 261.
11. M.R.J. Gibbs, J.E. Evetts, and J.A. Leake: *J. Mat. Sci.*, 1983, vol. 18, p. 278.
12. W. Primak: *Phys. Rev.*, 1955, vol. 100, p. 1677.

13. J.A. Leake, E. Woldt, and J.E. Evetts: *Mat. Sci. Eng.*, 1988, vol. 97, p. 469.
14. H.H. Liebermann: *J. Appl. Phys.*, 1987, vol. 61, p. 319.
15. "The Ultra Efficient Alternative: Amorphous Metal Transformers . . .": *GE Power Delivery and Control*, Transformer Business Department, General Electric Co., Hickory, North Carolina, 1989.
16. Data for the silicon steels were obtained from P.M. Curran, Allied-Signal Inc.
17. H.E. Wegner: *Moving to METGLAS (An Allied-Signal Publication)*, 1988, vol. 1.